Original Article

Bulletin of Pure and Applied Sciences.
Vol.36 D (Physics), Issue (No.1) 2017: P.15-25
Print version ISSN 0970 6569
Online version ISSN 2320 3218
DOI 10.5958/2320-3218.2017.00003.3

Power Petition of Nanotubes

Tarun Kumar Mathur and Dr. S.K. Srivastava

Tarun Kumar Mathur
Ph.D. Scholar, Department of Physics, Mewar Institute, Ghaziabad (U.P.)

Dr. S.K. Srivastava
Professor, Department of Physics, IMSEC, Ghaziabad (U.P.)

Corresponding author:
Dr. S.K. Srivastava
Professor,
Department of Physics,
IMSEC, Ghaziabad (U.P.)

E-mail: suyashkumar.srivastava@gmail.com

Received on 31.03.2017,
Accepted on 27.05.2017

Abstract:

Carbon nanotubes have been found to possess a wide variety of extremely remarkable properties, most notably high electrical and thermal conductivity, mechanical strength, and catalytic surface area. These properties contain carbon nanotubes with tremendous potential for a variety of power generation and storage devices including: lithium-ion (Li^+) batteries, polymeric solar cells, proton exchange membrane (PEM) fuel cells, and thermionic power devices, the key issues surrounding synthesis, characterization, and processing of carbon nanotubes in relation to device fabrication will be highlighted. Result on a variety of prototype devices which are being developed by the Nano power Research Laboratories (NPRL)at RIT in collaboration with researchers at the NASA Glenn Research Center will be presented.

Keywords: SWNT, MWNT, Fuel Cell Battery, Salon Cell, Thermionic emission

INTRODUCTION

They were first imaged by Iijima in 1991, carbon nano-tubes have generated an interest amongst scientists and engineers that surpasses almost any material known to man (1) The unique mechanical and electronic properties of both the single wall and multi-walled varieties of carbon nanotubes have proven to be a rich source of new physics and have led to applications in a wide variety of materials and devices (2) Carbon nano-tubes can be a rolled up graphene sheet, or multiple sheets as a rolled up graphene sheet, or multiple sheets as in the case of a multi walled nanotubes. The role up vector will determine the so-called in 'chirality' of the single wall carbon nanotubes (SWNT) relates to whether the structure will be metallic or semiconducting. The optoelectronic properties of a SWNT, will depend directly on

this choral angle, as well as the diameter of the nanotubes. In some cases, the π-orbital overlap can lead to a metallic SWNT which acts as a one-dimensional ballistic conductor. Other chiral angle exhibits the electronic energy transition similar to traditional semiconductor. Other chiral angle exhibits the electronic energy transition similar to a traditional semiconductor with band gap energy.

The synthesis conditions (temperature, pressure, carrier gas, etc.), metal catalyst type (Most commonly iron, nickel, cobalt, or yttrium), and carbon source (graphite or hydrocarbon) have all been shown to influence the properties of the resulting carbon nanotubes. Characteristic of multi-walled carbon nanotubes (MWNTs) are the concentric grapheme layers spaced 0.34 nm apart, with diameters from10 to200 nm & length up to hundreds microns. In the case of SWNTs the diameter typically ranges from 0.4 to 2 nm, and recently lengths up to 1.5 cm have been reported. The extra ordinary conductivity of carbon nanotubes (electrical = $10^4 S/cm$ and thermal = $6600 W/mK$ for a (SWNT. It is remarkable conductivity along with the extremely high Specific surface area (up to~1600 m^2/g) of carbon nanotube which has generated so much interest for their use in various power applications.

In particular, carbon nanotubes are showing tremendous promise in improving the performance of power devices, such as thin film polymeric solar cells, direct-methanol fuel cells lithium-ion (Li^+] batteries, ultra capacitors, and thermionic power supplies. In many of the power applications, the carbon nanotubes are used in concert with other materials (i.e. Nafion™ for PEM fuel cells, poly (3-octylthiophene) (P3OT) for thin film photovoltaic solar cells, or polyacrylonitrile in Li^+ batteries), often as a composite thin film. Data on the synthesis and characterization of laser-synthesized SWNTs and injection-CVD grown MWNTs, and highlight the importance of material standardization for power applications. Demonstration of the fabrication, testing, and analysis of PEM fuel cells, polymeric solar cells, Li^+ batteries and thermionic emitters, will illustrate the viability of carbon nanotubes in power applications.

EXPERIMENTAL

Single wall carbon nanotubes (SWNTs)

Single wall carbon nanotubes were synthesized using the pulse laser vaporization technique, employing an Alexandrite laser (755 nm). The raw SWNT soot was collected from the condensed region on the quartz tube at the rear of the furnace. Purification of raw SWNT soot was performed using modifications of the previously reported procedure. in summary, approximately 50 mg of raw SWNT soot was brought to reflux at 125°C in 3 M nitric acid for 16 h and then filtered over a I μm polytetrafluorothylene (PTFE) membrane filter with copious amounts of water. The filter paper was rinsed consecutively with acetone, ethanol, 2.5 M NaOH, and H_2O until filtrate became colorless after each step. The membrane filter was dried at 70° C in vacuole to release the resulting SWNT paper from the filter paper. The SWMT paper was thermally oxidized in air at 550° C for 1 min in a thermolyne 1300 furnace. Finally, a 6 M hydrochloric acid wash for 60 min using magnetic stirring, with similar filtering steps and thermal oxidation at 550° C for 20 min completed the purification.

Multi-wall carbon nanotubes (MWNTs)

In summary, toluene solutions of the catalyst precursor were injected into the first zone of a two zone furnace using a syringe pump. The temperature of zone one was held above the boiling point of the solvent and above the decomposition temperature of the precursor. A mixed carrier gas of hydrogen and nitrogen carried the reaction products into the hot zone of the furnace. The MWNTs deposited on the walls of the fused silica reactor tube, just inside the entrance of the hot zone.

Act of characterizing

Analysis of the carbon nanotubes was performed by scanning electron microscopy (SEM), transmission electron microscopy (TEM), Raman spectroscopy, optical absorption spectroscopy, thermo gravimetric analysis (TGA), and surface area analysis. The SEM was conducted using a Hitachi S-900, with samples applied directly to the brass stub using silver paint. The instrument operated at an accelerating voltage of 2kV and magnifications ranged from 5000 to 250,000×Raman Spectroscopy was performed at room temperature using a JY-Horiba Labrum spectrophotometer with excitation energy of 1.96 eV. Thermo gravimetric analyses (TGA) were conducted using a TA Instruments 2950. Samples were placed in the platinum pan balance in quantities of ~1 mg and ramped at 10°C/min from room temperature up to 950°C under air at a gas flow rate of 60 scum and $N_{2(g)}$ balance purge at a gas flow rate of 40 scum. Surface area analysis was conducted with a Quanta chrome NOVA 1000e at 77 K under $N_{2(g)}$.

Manufacture of Device with testing

Preparation of PEM fuel cell membranes for testing consisted of dispersing 64 mg do pant with 5mL Nafion solution (5%(w/w) in lower aliphatic alcohols). The dispersions were ultrasonicated at 40°C for 2 h and then poured into square 16cm^2 PTFE coated aluminum forms and allowed to dry slowly in air until all of the solvents had evaporated. The fuel cell testing apparatus consisted of H-TEC PFMFC® Kit. This includes two Plexiglas blocks containing gas ports and two 16 cm^2 metal grid electrodes with an elastomeric rim which functions as an air and gas seal. Sandwiched between the electrodes were the anode catalyst membrane, the proton exchange membrane (Nafion 117, 0.007 in thick) and the cathode catalyst membrane. Before use membrane, were hydrated and the whole fixture bolted together. The reference membrane was the commercially supplied membrane from H-TEC. Fuel ceils performance data were acquired with a Kejthley 237 high Voltage source measurement Unit, over a current range of 10^{-6} to 10^{-1} A, at 25°C and atmospheric pressure.

Polymeric solar cells were fabricated from SWNT-P3OT composite solutions based on a series of mixing. The lithium-ion (Li^+) batteries were characterized in a typical coin cell configuration using a carbon nanotubes 'Paper' as the anode and a conventional thin film polymer as cathode. The thin film polymer cathode consisted of 70 % (w/w) of Merck SNC 8020 $LiNi_{0.12}Co_{0.8}O_2$ and 10% (w/w) Superior Graphite Inc. LBG 80 graphite in 20 % (w/w) of polyvinylidene fluoride (PVDF). The cathode was prepared by pipe ting $LiNi_{0.2}Co_{0.8}O_2$ and PVDF mixture dissolved in 1-methyl-2-pyrrolidone (NMP) directly into the coin cell cathode cap and dying overnight in a Vacuum oven at 60°C. The battery was charged using a constant current of 100 µA/cm^2 until it reached a voltage of 4.2 V at which point it was switched over to a 100µA/cm^2 discharge current. The battery was then discharge to a voltage of 2.0 V at which point it was switched to charging once again. Thermionic testing involved using two different samples: (1) purified SWNT paper, and (2) MWNTs grown directly on a tantalum substrate. The tantalum anode was maintained at a distance of 500µm from the retainer. The tantalum retainer was controllably heated using a boron nitride heater while the voltage was ramped at 10 V increments from 0 to 1100V.

FACTS ABOUT CARBON NANOTUBES

Property, Characterization and Artificial Product of Carbon Nanotubes

Impurities include metal catalysts, amorphous carbon, fullerenes, and other graphitic materials. Also, the presence of carbon 'coatings or encapsulated metal particles can be problematic during characterization or purification steps. Scanning electron microscopy (SEM) and transmission electron microscopy (TEM) images for raw and purified laser-generated SWNTs. Evident from both techniques are the presence of the synthesis by-

products and the bundling of SWNTs due to the Vander Wall's interactions along the side walls of the materials. The ability to identify the presence of material components in SWNT-containing samples using microscopy is extremely vital, including a qualitative assessment of the purity and quality of the material. However, current work is advancing our understanding to accurately quantify the respective mass fractions of each component in a given sample, which is imperative for material standardization in power applications.

For the synthesis and characterization of multi-walled carbon nanotubes (MWNTs) as well, although the material properties are slightly different. MWNTs can be synthesized with various metal catalyst-carbon source schemes, but typical approaches have been the 'floating catalyst' CVD method and the injection CVD method. Our recent result using the injection CVD method with a precursor of cyclopentadienyliron dime dicarbonyl have shown high MWNT crystalline, with low metal catalyst impurities, minimal structural defects, and reduced amorphous carbon impurities. The raw MWNT (see Fig. 2) can exist as an entangled network or with a preferential orientation, depending on the synthesis conditions. The physical properties associated with carbon nanotubes, like diameter distributions, length distributions, defect content, and bundling effects, are influential factors that may impact device performance. Spectroscopic techniques, like Raman and optical absorption can be used to accurately assess the diameter- distribution of SWNTS based on the diameter-dependent resonant Raman effects and the relation between optical band gap and SWNT diameter. 3a is an overlay of the Raman spectra for purified SWNTs and raw MWNT soot with incident laser energy of 1.96eV. The characteristic radial breathing mode (RBM) at low energy (100-300cm^{-1}) for the SWNTs is used to calculate the diameter distribution based on Eq, (1), The following relationship between diameter (d,nm) and Raman shift (wrbm,cm^{-1}) has been reported for bundled SWNTs:

$$wrBM = \frac{224}{d} + 14$$

For our typical laser vaporization conditions, the diameter range is between 1.2 and 1.4nm. It is important to note that contrast to the current MWNT sample where the innermost diameters were observed by TEM to range from 3 to 30 nm, it has been shown that a RBM can be observed for MWNT samples with very thin innermost tubes (~1 nm).

Optical absorption spectroscopy is another technique for evaluating the diameter distribution of SWNTs, since the optical transitions are based on the discrete electronic transitions associated with the Van Hove singularities of the semicon-ducting and metallic types [35]. The ith pair of discrete electronic transition energies corresponding to these singularities is approximated by the following:

$$^{S,M}E_{ii} = \frac{2nac\text{-}c\gamma}{dswnt}$$

Where n is an integer, having values of 1,2,4,5, or 7 for semiconducting (S) SWNTs and n=3 or 6 for metallic (M) SWNTs in the spectral range of interest ac-c the carbon-carbon bond distance with a value of 0.142 nm, and dawns the SWNT diameter. The carbon-carbon overlap integral or SWNTS has been reported to range from 2.45 to 3.0 eV. Therefore, neither Raman nor optical absorption spectroscopy is capable of outer diameter analysis for the current sample of injection CVD MWNTs, and the microscopy approach provides the only current method for assessment. The diameters ranged from 9 to 92 nm and had an average of 44+ 22 nm. Carbon nanotubes can further enable the aspect ratio (length/diameter) to be calculated. The aspect ratio is an important parameter for ceramic or polymer composite applications where structural, thermal, and/or electrical conductivity enhancement is desired. Microscopic analysis has been the prominent method of estimating the length distribution with electron micrographs and AFM images being routinely used . For the laser-generated SWNTs, the typical length scale is ~1-10μm, giving an aspect ratio for individual

SWNTs of 1000-10,000. In comparison, the injection CVD MWNTs having a similar length scale would have an aspect ratio from 10 to 1000, since the diameters are significantly larger. Qualitative estimation of the defect density in both SWNTs and MWNTs is performed using a combination of microscopy and Raman spectroscopy. Raman spectroscopy has also been used for establishing the defect density based on the relative ratio of the D-Band (~1350cm^{-1}) intensity to the G-Band (~1600 cm^{-1}). The D- Band is the Raman mode associated with a disorder-induced dispersion relation which indicates the presence of vacancies or non-aromatic sites in the graphitic structure. Evident from the Raman spectra in a are the corresponding D- and G-Bands for SWNTs and MWNTs. The relative peak ratios can be qualitatively assigned to the defect density in the samples, thus showing a higher defect density in the MWNTs compared to the SWNTs.

We have observed such defunding effects previously in SWNT- Nafion polymer composites where a factor of five reduction in average Additionally, unbundling effects can be probed using Raman spectroscopy by monitoring the Raman shifts in the RBM or changes in the line shape associated with the Bruit-Wigner-Fano (BWF) lineshape of the G-Band. (TGA) to monitor. TGA overlay for raw SWNT soot, purified SWNTs, and raw MWNT soot. The highest decomposition transition is apparent for the purified SWNTs, evidence for the stability of its highly crystalline structure.

Determination of the actual metal impurity content can be performed by adjusting the high temerity content can be performed by adjusting the high temperature residue based on the oxidation products of the metal catalysts. However, since both SWNTs and MWNTs are deposited on quartz substrates during synthesis, the occasional presence of SiO_2 can influence these calculations and the proper adjustment is made with quantitative energy dispersive X-ray spectroscopy (EDS). Such TGA residue values are important since certain applications require ceramic or polymer composites containing carbon nanotubes, and evaluation.

The specific surface area is an attractive property of carbon nanotubes that is anticipated to improve many applications like fuel cells, batteries, and capacitors, which rely on this attribute for performance Bruner-Emmett-Teller (BET) specific surface areas values were measured to equal 720, 1200, and 1252 m^2 / g, respectively. There are also variations in the adsorption and desorption curves for SWNTs which are not present in the case of MWNTs.

Chemical Preparation of Carbon nanotubes

In certain applications, the need to modify the carbon nanotubes structures may be necessary to improve device performance. Through oxidative acid treatments, the sidewalls and end caps of carbon nanotubes can react to produce carboxylic-acid functionalized materials. The desire to 'cut' the carbon nanotubes can be performed by oxidative acid conditions in the presence of ultrasonication. The resulting material contains shortened nanotubes with openings for ion or gas intercalation. These materials are expected to improve power applications, such as Li^+ batteries or hydrogen storage for PEM fuel cells.

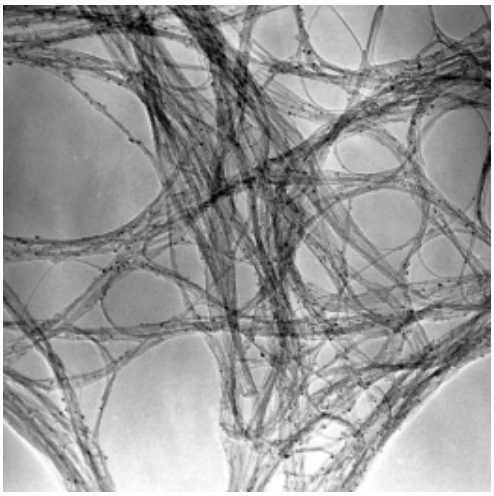

Example of purified SWNTs that were cut using an ultrasonication step in the presence of 4:1 mixture concentrated H2So4:H2O2 .The abundance of SWNT ends in verification to the efficacy of this procedure, since the presence of nanotube ends in a SEM image at this magnification is rare for raw or purified SWNTs.

Certain power applications require exotic active materials to promote catalysis or improve efficiencies in the device. Laser vaporization is the ability to tailor the metal catalyst during synthesis to selectively enrich the resulting SWNT- product. Fuel cell applications routinely use platinum as the electrode catalyst whereas other metals like ruthenium, rhodium, or palladium, are often used for other electrochemical reactions. The common cathode material in LI^{+} batteries is $LiNi_{0.2}Co_{0.8}O_2$ which could be replaced or mixed with nickel-cobalt enriched SWNTs that would improve the electrical conductivity in the cathode material. Such ideas are presently being developed with our recent ability to selectively remove the majority of non SWNT carbon impurities.

Construction of Carbon nanotubes

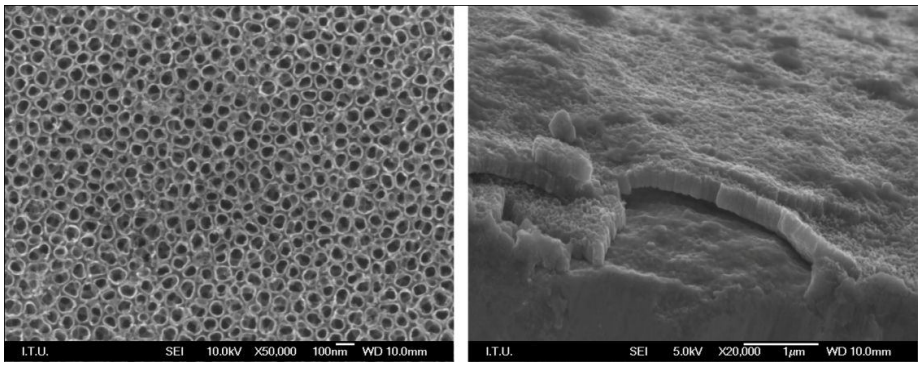

Successful dispersion of SWNTs into the Nafion nonnumeric polymer, most commonly used for proton exchange membrane (PEM) fuel cells and electrochemical actuators.

The cross-sectional SEM images from both 5% (ww) MWNT and 5 % (w/w) SWNT-Nafion composites. Evident from the images is the homogeneous distribution of do pant materials in the thin films. When the SWNT opadnt is desired to increase the electrical conductivity in the polymeric films. In fact, displayed in Fig. 8 is a conductivity plot which shows how modest doping levels of purified SWNTs can dramatically improve the electrical conductivity in a Nafion composite material [10]

ROLL OF CARBON NANOTUBES IN POWER USES

Membrane fuel cells due to proton exchange

The limiting factors of device performance which may be addressed through carbon nanotubes incorporation are the enhanced oxidation of $H_{2\,(g)}$, electron transport from anode to cathode, and reduction of $O_{2\,(g)}$. The current technology uses platinum supported carbon-powder (such as E-TEK Vulcan XC- 72) based electrodes to promote these processes, although recent work has shown the potential for platinum supported MWNTs as viable materials. Our work has sought to perform side-by-side comparisons between the conventional E-TEK materials and carbon nanotubes. Construction of 20% (w / w) dopant- Nafions composite membranes incorporating E-TEK, 50:50 mix of raw SWNT soot and E-Tec have been fabricated. Displayed in is a digital image of a typical 16 cm^2 membrane which is tested using a commercially available H-TEK system under 1 atom $H_{2\,(g)}$ and $O_{2(g)}$ at 25°C.

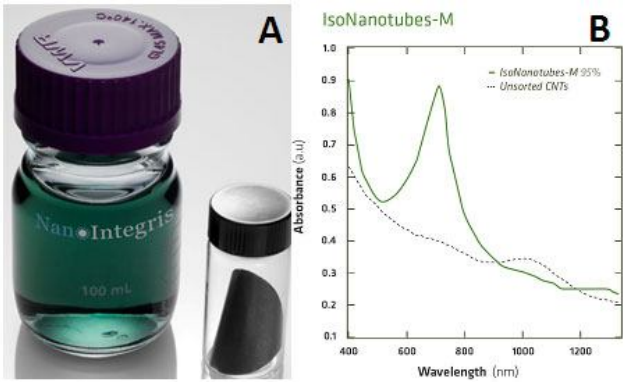

Polymorphism Solar Cells

Single wall carbon nano-tubes have recently been incorporated into poly (3-octylthiophene) (P3OT) to promote exaction dissociation and improve electron transport in a polymeric solar cell. When the polymer is placed in a properly structured device with a suitable do pant to promote dissociation of the exaction and conduction of the electron, hole conduction proceeds through the polymer and contributes to an overall photocurrent. The use of SWNTs in these polymers is an appropriate doe's pant choice since the electron affinity is higher for SWNTs compared P3OT and the electron transport in a metallic SWNT is typical of a ballistic conductor. Devices were fabricated by spray deposition of a 0.1% (w / w) dispersion of purified SWNTs in P3OT onto indium-it-oxide (ITO) coated ply(ethylene terapthalate) (PET). The photovoltaic response was measured under 1 Sun air mass zero (AM0) illumination at 20°C. The current-voltage curve for the 0.1% (w / w) SWNT-P3OT composite is shown in Fig.

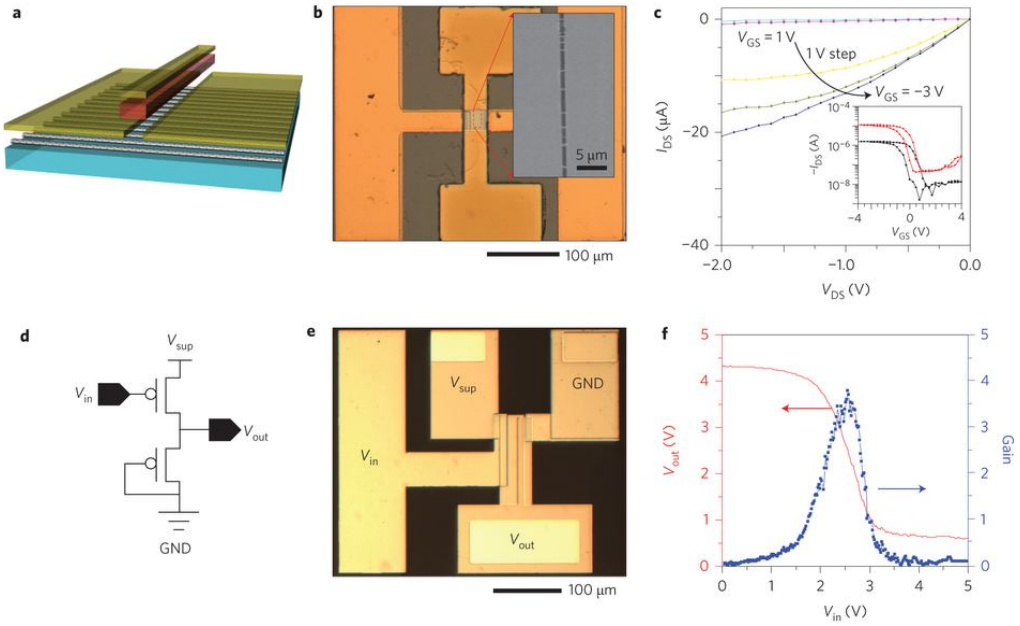

The high open-circuit voltage (V_{oc}) of 0.85 V is typical of these devices with other SWNT-P3OT devices having exhibited values up to 1.0 V [16]. There is also a dramatic improvement in the shot-circuit current (I_{sc}) for the AM0 illuminated response compared to the dark current. This response translates into an overall power conversion efficiency which is still very low compared to traditional crystalline solar cells.

Batteries, made from Lithium Z-ion (Li^+)

Evaluation of carbon nanotubes for Li+ batteries has been an appropriate pursuit since the anode has been conventionally constructed from graphite. Lithium-ion batteries rely on the efficient cycling of Li^+ between the cathode and anode where rapid charging, high ionic storage, and slow discharge constitute ideal device characteristics. Coin cell batteries which were constructed using a purified SWNT 'paper' as the anode and a mixture of 70% (w/w) $LiNi_{0.2}Co_{0.8}O_2$ 10% (w/w) LBG 80 graphite, and 20% (w/w) polyvinylidene fluoride (PVDF) as the cathode were tested. (1) cathode mixture in aluminum cap, (2) Calgary 10,10)separator, (3) O-ring, (4) SWNT anode, and (5) stainless still cell base.

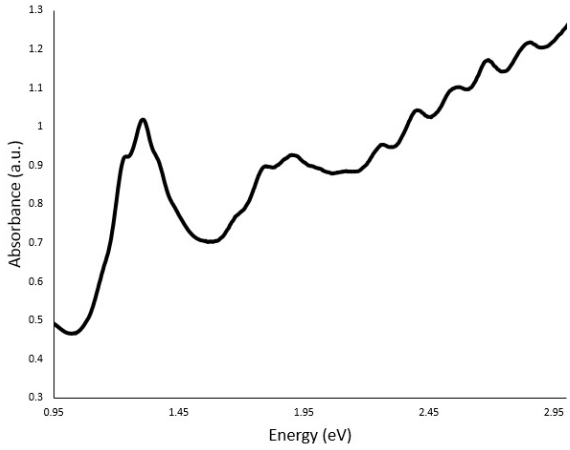

Shows the typical charge / discharge behavior for the SWNT anode coin cell which was tested at 25°C and a constant current of 100 μ A / cm^2.

Thermionic emitters

Carbon nanotubes are currently being investigated for possible thermionic applications due to their potentially low work function (which can be chemically modified), their ability to be produced in aligned arrays, and their nanoscale tip geometry based on their diameters. Thermionic emission is a process where an increase in temperature will promoter electron tunneling through a micro scale vacuum gap from a low work function emitter to an appropriate collector (1) application of purified carbon nanotubes to a metal retainer, (2) carbon nanotubes grown directly on a metal retainer by CVD, (3) carbon nanotubes incorporated into a matrix (ceramic or epoxy) and applied to the metal retainer. The effect of field assisted thermionic emission is observed at higher voltages as well with the highest performance from the carbon nanotubes grown on tantalum. The inset plot shows the emission data at zero bias in relation to the Richardson- Dutchman equation for the constant collector area [15]. The resulting slope for both purified SWNTs and MWNTs grown on tantalum indicates a calculated effective barrier height to thermionic emission equal to 1.2 eV.

RESULT

Carbon nanotubes represent a class of exciting new materials with extraordinary electrical, thermal, and mechanical properties. Taking advantage of these intrinsic properties relies on the ability to systematically synthesize, characterize, and integrate standardized materials into actual devices. Appropriate characterization of the properties (diameter, length, purity, surface area, bundling, etc.) has been highlighted with microscopic, spectroscopic, thermal, and surface area analysis, showing the importance of these techniques in moving towards material utilization.

The ability to employ post-synthesis processing steps on carbon nanotubes whereby chemical modification, metal catalyst retention, or dispersion in polymer and ceramic composites is an attractive approach to device fabrication has been shown. Functional devices using carbon nanotubes were demonstrated for power applications, such as PEM fuel cells, polymeric solar cells, Li^+ batteries, and thermionic emitters.

Acknowledgements

The authors *acknowledge* ***T*arun Kumar Mathur** Research Scholar Mewar for the TEM studies, for TiO_2 coating of nanotubes for thermionic for the thermionic emission measurements.

REFERENCES

1. S. Iijima, nature 354 (1991) 56.
2. H. Dai, Surf Sci, 500 (2002) 218-241.
3. T. Guo, P. Nikolaev, A.G. Ringlet, D. T. Colbert, R.E. Staley, J. Phys. Charm, 99 (1995) 1694, 10697.
4. A.C. Dillon, P.A. Parilla, J.L. Aleman, J.D Perkins, M.J. Hebe, Chem. Phys. Letts. 316 (2000) 13-18.
5. E. Munoz, W.K. Maser, A.M. Benito, M.T. Martinez, G.F. de la Fuente, A, Righi, E. Anglaret, 6. J.L. Sauvajol, Synth, Mct. 121 (2001) 1193-1194.
6. S. Huang, M. Woodson, R. Smalley, s, 4 (2004) 125-1028.
7. A. Thes, R.Lee, P. Nikolayev, H. Dai, P. Petit, J. Robert, C. Xu, Y.H. Lee, S.G. Kim, A. Rinzler, 9. D.T. Colbert, G. Suzerain, D. Tomean, J.E. Fischer, R. Smalley, Science 273 (1996) 483-487.
8. S. Berber, Y.-K. Kwon, D. Tomanek, Phys. Rev. Lett. 84 (2000) 4613-4616.

9. M.J. Biercuk, M.C. Llaguno, M. Radosavljevic, J.K. Hyun, A.T. Johnson, J.E. Fischer, Appl. Phyus. Lett. 80 (2002) 2767-2769.
10. B.J. Landi, R.P. M.J. Hebe, J.L. Alleman, W. VanDerveer, T. Gennett, Nano Letts. 2 (2002) 1329-1332.
11. R. H. Baughman, C. Cui, A.A. Zakhidov, Z. Irbil, J.N. Barisci, G.M. Spinks, G.G. Wallace, A. 15. Mazzoldi, D. De Rossi, A.G. Rinzler, O. Jaschinski, Stroh, M. Kermes, Science 284 (1999) 1340-1344.
12. E. Kymakis, G.A.J. Amratunga, Appl. Phys. Lett. 80 (2002) 112-114.
13. W,Li, C. Liang, W. Zhou, J, Qiu, Z. Zhou, G. Sun, Q, Xin, J. Phys. Chem. B 107 (2003) 6292-6299.
14. E. Frackowiak, F. Beguin, Carbon 40 (2002) 1775-1787.
15. M.-C. Kan, J.-L. Huang, J.C. Sung, K.-H. Chen, B.-S. Yau, Carbon 41 (2003) 2839-2845.
16. B.J. s R. P. Raffaelle, S. L. Castro, S.G. Bailey, Prog. Photo- Votaics: Res Appl., in press.
17. J.D. Harris, A.F. Hepp, R.P Raffaelle, T. Gennett, R. Vander Wall, B.L. Landis, Y. Leo, D.A. Shearson, Growth and characterization of multi- walled carbon nanotubes at NASA 23. Glenn Research Center, in: Proceedings of the First International Energy Conversion 24. Engineering conference, Portsmouth, VA, 2003.
18. G.S. Duesberg, J. Muster, H.J. Byrne, S. Roth, M. Burg hard, Appl. Phys. A 69 (1999) 269-274.
19. R.C. Haddon, J. Sippel, A.G. Rinzler, F. Papadimitrakopoulos, MRS Bull. 29 (2004) 252-259.
20. A.C. Dillon, T. Gannett, K.M. Jones, J.L. Aleman, P.A. Padilla, M.J. haven, Adv. Matter. 11 (1999) 1354-1358.
21. B.J. Landis, H.J. Ruff, C.M. Evans, R.P. Raffaelle, Purity assessment of as-produced single wall carbon nanotubes soot, nil proceedings of an International Conference on Carbon, Carbon 2004, Providence, RI, 2004.
22. S. Huang. L. Dai A.WH. Mau. J. Phys. Chem. B 103 (1999) 4223-4227.
23. B.C. Satishkumar, A. Govindaraj. C.N.R. Rae, Chem. Phys. Leu. 307 (1999) 158-162.
24. C Singh, T. \Quested, C.B. Boothroyd, P. Thomqas, I.A. Kinloch, A.I. Abou-Kandil, A.H.. Windle, J. Phys. Chem. B 106 (2002) 10915-10922
25. Z. Zhou, L. Ci, X. Chen, D. Tang, X. Yan, D. Liu, Y. Liang, H. Yuan, W. Zhou, G. Wang. S. Xie, Carbon 41 (2003) 337-342.
26. R. Andrews, D. Jacques, A.M. Rao, F. Derbyshire, D. Qian, X. Fan, E.C. Dickey, J. Chen, Chem. Phys. Lett. 303 (1999) 467- 474.
27. A. Cao, L. Ci, G. Wu, B. Wei, C. Xu, J. Liang, D. Wu, Carbon 39 (2001) 152-155.
28. E.C. Dickey, C.A. Grimes, M.K. Jain, K.G. Ong, D. Quian, P.D. Kichambare, R. Andrewes, D.. Jacques, Appl. Phys. Lett. 79 (2001) 4022-4024.
29. R. Kamalakaran, M. Torrones. T. Seeger, P. Kohler-Redlich, M. Ruhle, Y.A. Kim, T. Hayashi, M. Endo, Aook. Phys. Lett. 77 (2000) 3385-3387.
30. M. Mayne, N. Grobert, M/ Terrones, R. Kamalakaran, M. Ruhle, H. W. Kroto, D.R.M. Walton, Chem. Phys. Lett. 338 (2001) 101-107.
31. C. Singh, M.S.P. Shaffer, A.H. Windle, Carbon 41 (2003) 359-368.
32. C. Singh, M.S.P. Shaffer, A. H. Windle, Carbon 41 (2003) 359-368.
33. B. Wei, R. Vajtai, Y.Y. Choi, P.M. Ajayan, H. Zhu, C. Xu, D. Wu, Nano LEtt. 2 (2002) 1105-1107.
34. H.W. Zhu, C.L. Xu, D.H. Wu, B.Q. Wei, R. Vajtai, P.M. Ajayan, Science 296 (2002) 884-886.
35. H. Kataura, Y. Kumazawa, Y. Naniwa, I. Umezu, S. Suzuki, Y. Ohtsuka, Y. Achiba, Synth. Met. 103 (1999) 255-2558.
36. A. M. Rao, J. Chenn, E. Richer, U. Schlecht, P.C. Eklund, R.C. Haddon, U.D. Venkateswaran, Y-K. Kwon, d. Tomanek, Phys. Rev. Lett. 86 (2001) 3895-3898.
37. X. Zhao, Y. Ando, L.-C. Qin, H. Kataura, Y. Naniwa, R. Saito, Chem. Phys. Lett. 361 (2002) 169-174.
38. Y. Lian, Y. Maeda, T. Wakahara, T. Akasaka, S. Kazaoui, N. Mi- name, N. Choi, H. Tokumot, J. Phys. Chem B 107 (2003) 12082- 12087.
39. T.W. Odom. J.-L Huang. P. Kim, C.M. Lieber, Nature 391 (1998) 62-64.

40. J.W.G. Wilder, L.C. Venema, A.G. Rinzler, R.E. Smalley, C. Dekker, Nature 391 (1998) 59-62.
41. A. Hagen, T. Hertel, Nano Lett. 3 (2003) 383-388.
42. B.J. Landi, H. J. Ruf, J.J. Worman, R. P. Raffaelle, J. Phys. Chem. B 108 (2004) 17089-17095.
43. M.J. O'Connell, S.M. Bachilo, C.B. Huffman, V.C. Moore, M.S. Strano, E.H. Haroz, K.L. Rialon, P.J. Boul, W.H. Noon, C. Kittrell, J. Ma, R.H. Hauge, R.B. Weisman, R.E. Smalley, Science 297 (2002) 593-596.
44. C.A. Furado, U.J. Kim, H.R. Gutierrez, L. Pan, E.C. Dickey, P.C. Eklund, J. Am. Chem. Soc. 126 (2004) 6095-6105.
45. M.Endo, Y.A. Kim, Y Fukai, T. Hayashi, M. terrones, H. Terrones, M.S. Dresselhaus, Appl.Phys. Lett. 79 (2001) 1531-1533.
46. M.S. Dresselhaus, G. Dresselhaus, A. Jorio, A.G. Souza Filho, R. Saito, Carbon 40 (2002) 2043-2061.
47. N. Bendiab, R. Almairac, M. Pailet, J. L. Sauvajol, Chem. Phys. LEtt. 372 (2003) 210-215.
48. J. Liu, A.G. Rinzler, H. Dai, J. J. Hafner, R.K. Bradley, P.J, Boul, L.A.T. Iverson, K. Shelimov, 56. C.B. Huffman, F. Rodriguez-Macias, Y.S. Shon, T.R. Lee, D.T. Colbert, R. E. Smalley, Science 280 (1998) 1253-1256.
49. B.J. Landi, H.J. Ruf, C.M. Evans, S.G. Baqiley, S.L. Castro, R.P. Raffaelle, Sol. Energy Mater. Sol. Cells in press.
50. J. Larminie, A. Dicks, Fuel Cell Systems Explained, Wiley, West Sissex, 2003.
51. H.J. Ruf, B.J. LKandi, R.P. Raffaelle, SWNT enhaced PEM fuel cells, in: proceedings of the second international Conference on Fuel Cell Science, Engineering, and Technology, Fuel Cell 2004, Rochester, NY, 2004.
52. B. Kannan, K. Catelino, A. Majumdar, Nano let. 3 (2003) 1729-1733.
53. A. Goetzberger, J. Luther, G. Willeke, Sol. Energy Mater. Sol Cells 74 (2002) 1-11
54. A. Wadhawan, R.E. Stallcup II, J.M. Perez, Appl. Phys. Lett. 78 (2001) 108-110.